LA-UR- 08-4299

Approved for public release; distribution is unlimited.

Title: Climatic implications of correlated Upper Pleistocene glacial and fluvial deposits on the Cinca and Gállego Rivers, NE Spain

Author(s): Claudia J Lewis
Eric V McDonald
Carlos Sancho
Jose-Luis Pena
Edward J Rhodes

Intended for: publication in the journal:
Global and Planetary Change

Los Alamos NATIONAL LABORATORY EST. 1943

Climatic implications of correlated Upper Pleistocene glacial and fluvial deposits on the Cinca and Gállego Rivers, NE Spain

Claudia J. Lewis[1*], Eric V. McDonald[2], Carlos Sancho[3], José Luis Peña[4], and Edward J. Rhodes[5]

[1] Earth & Environmental Sciences Division, MS D452, Los Alamos National Laboratory, Los Alamos, NM, 87545, USA; TEL: 1-505-665-7728; FAX: 1-505-667-1628; E-mail: clewis@lanl.gov
[2] Desert Research Institute, 2205 Raggio Parkway, Reno, NV, USA
[3] Departamento de Ciencias de la Tierra, Universidad de Zaragoza, Zaragoza, Spain
[4] Departamento de Geografía y Ordenación del Territorio, Universidad de Zaragoza, Zaragoza, Spain
[5] Laboratory of the Research Laboratory for Archaeology and the History of Art, University of Oxford, Oxford, UK; now at: Department of Environmental and Geographical Sciences, Manchester Metropolitan University, Manchester, UK

*Corresponding author

Abstract

We correlate Upper Pleistocene glacial and fluvial deposits of the Cinca and Gállego River valleys (south central Pyrenees and Ebro basin, Spain) using geomorphic position, luminescence dates, and time-related trends in soil development. The ages obtained from glacial deposits indicate glacial periods at 85 ± 5 ka, 64 ± 11 ka, and 36 ± 3 ka (from glacial till) and 20 ± 3 ka (from loess). The fluvial drainage system, fed by glaciers in the headwaters, developed extensive terrace systems in the Cinca River valley at 178 ± 21 ka, 97 ± 16 ka, 61 ± 4 ka, 47 ± 4 ka, and 11 ± 1 ka, and in the Gállego River valley at 151 ± 11 ka, 68 ± 7 ka, and 45 ± 3 ka. The times of maximum geomorphic activity related to cold phases coincide with Late Pleistocene marine isotope stages and Heinrich events. The maximum extent of glaciers during the last glacial occurred at 64 ± 11 ka, and the terraces correlated with this glacial phase are the most extensive in both the Cinca (61 ± 4 ka) and Gállego (68 ± 7 ka) valleys, indicating a strong increase in fluvial discharge and availability of sediments related to the transition to deglaciation. The global Last Glacial Maximum is scarcely represented in the south central Pyrenees owing to dominantly dry conditions at that time. Precipitation must be controlled by the position of the Iberian Peninsula with respect to the North Atlantic atmospheric circulation system. The glacial systems

and the associated fluvial dynamic seem sensitive to 1) global climate changes controlled by insolation, 2) North Atlantic thermohaline circulation influenced by freshwater pulses into the North Atlantic, and 3) anomalies in atmospheric circulation in the North Atlantic controlling precipitation on the Iberian Peninsula. Our model of glacial and fluvial evolution during the Late Pleistocene in northern Spain could be extrapolated to other glaciated mountainous areas in southern Europe.

Key words: glacial deposits; fluvial terraces; OSL dating; climate change; Pleistocene; Pyrenees.

1. Introduction

The Iberian Peninsula is located in a pivotal geographic position that is highly sensitive to climatic perturbations in the North Atlantic. Some investigators have proposed, from paleoclimate marine proxies in the western Mediterranean area, a link between North Atlantic circulation and weather in Iberia (e.g., Cacho et al., 2000; Sánchez-Goñi et al., 2002; Bout-Roumazeilles et al., 2007). What is lacking, however, is a robust determination of the timing of Pleistocene cold stages on the Iberian peninsula and their consequences in terms of glacial and fluvial sedimentary deposits.

Until now, few chronologic data have been available to pin down the timing and extent of major Pleistocene glaciations in any of the mountain ranges of southern Europe (e.g., Hughes et al., 2006a, b). Furthermore, the timing of maximum ice extent is a controversial topic. The global Last Glacial Maximum (LGM) is associated with a major advance of glaciers in some parts of northwest Europe, and it is generally agreed that maximum cold occurred at 20-18 ka (e.g., Bowen et al., 1986). However, this does not represent the timing of the maximum extent of glaciers in either the northern or southern Pyrenees (Hérail et al., 1986; García-Ruiz et al., 2003;

Sancho et al., 2003, 2004). The LGM in the Pyrenees began as early as 50-60 ka and ended around 18 ka (Pallás et al., 2006). Only in the eastern Pyrenees did the maximum ice advance occur during the LGM (Delmas et al., 2008) .

Chronological control on Pleistocene fluvial terrace development in southern Europe is somewhat better (Macklin et al., 2002), especially on the Iberian Peninsula (Santisteban and Schulte, 2007). Major fluvial aggradation events appear to correlate across the Mediterranean basin and may be synchronous with climate changes (Macklin et al., 2002). However, compiled chronological data for Iberia suggest each river system may respond differently to local and regional climate control and other effects (Santisteban and Schulte, 2007).

The Cinca and Gállego are major rivers of northern Spain with their headwaters in the highest part of the Pyrenean range (Fig. 1). Their river valleys preserve excellent records of glacial episodes and periods of fluvial incision and aggradation (Sancho et al., 2004). Moraines and fluvial terraces from this area provide a means of dating cold periods in the Pyrenees for comparison with the few dated glacial and fluvial deposits from other areas in Europe and to proxy records of climate change.

In this paper, we present chronological data on Upper Pleistocene glacial and fluvial deposits from valleys in the south central Pyrenees and Ebro basin, analyze the response of glacial and fluvial systems to climate change, and relate the climate signal evident in northern Spain to climatic changes recorded in both the Mediterranean and the North Atlantic. The chronology of valley glacier dynamics and the associated fluvial response in areas of southern Europe may have implications for our understanding of the effects of global climate change on the continents.

2. Study area

Numerous moraine remnants preserved in the headwaters of the Cinca and Gállego Rivers demonstrate that the length of valley glaciers surpassed 35 km, and the thickness of ice exceeded 500 m in some localities (Chueca et al., 1998). In addition, fluvial terraces are well preserved and easily recognized along the valleys of the Cinca and Gállego Rivers. Strath terraces comprise the dominant terrace type on both rivers (Sancho, 1988; Benito, 1989). Terrace deposits in the vicinity of terminal moraines in many cases show signs of fluvioglacial activity, providing a direct link between glacial episodes and fluvial terrace formation.

We have studied the fluvial terraces of the Cinca River (Fig. 1) along the entire length of its valley (~170 km long) and the terraces of the Gállego from the headwaters to the town of Gurrea (~130 km) in the Ebro basin; below Gurrea, thick composite fill terraces related to gypsum bedrock dissolution obscure relations near the Gállego's confluence with the Ebro River (Benito et al., 1998). On both the Cinca and Gállego, broad terrace treads (paleochannels of a braided stream) are underlain typically by <2-10 m of largely cobble-sized gravels in a sand matrix with sparse sand lenses. Terrace deposits also contain large (20-100 cm diameter) rounded boulders. Separation between adjacent strath terraces ranges up to 40 m, facilitating mapping and measurement of the straths and the alluvial deposits that overlie them. Along both rivers, straths are carved into Paleozoic basement, Cretaceous to Eocene marine strata of a previous extensional episode, and Eocene to Miocene Pyrenean synorogenic marine strata along the mountain reaches and Eocene to Miocene synorogenic continental strata along the Ebro basin reach.

3. Material and methods

Geomorphic mapping on an aerial photographic base (1:18,000 scale), soils analysis, and numeric dating were carried out as part of this study. Mapped terrace remnants were extensively field checked.

We used optically stimulated luminescence (OSL) techniques to date the following: 1) sand lenses within glacial till, 2) well-sorted fluvial sands from lenses within massive gravel deposits, 3) overbank deposits on top of the gravels, and 4) eolian silt on top of terrace deposits. We used standard sampling techniques for poorly lithified materials, sampling with plastic and metal tubes or under a light-tight black plastic sheet into plastic bags that were then wrapped in aluminum foil. Sample preparation and OSL measurements were carried out at the Luminescence Dating Laboratory of the Research Laboratory for Archaeology and the History of Art (University of Oxford, UK) and the Luminescence Dating Laboratory of the Research School of Earth Sciences (The Australian National University, Australia). Sand-sized quartz was extracted using the methodology described by Rhodes (1988), which includes sieving, concentrated hydrofluoric acid treatment, and density separation of heavy minerals using sodium polytungstate solution. OSL dating was based on a single aliquot regenerative-dose (SAR) protocol (Murray and Wintle, 2000, 2003), using a Risø TL-DA-15 automated luminescence reader. For the majority of the samples, the dose rate is based on in situ gamma ray spectrometry. For a few samples, beta and gamma dose rate were estimated using neutron activation analysis (NAA) of sediment U, Th and K content, and cosmic dose rates were calculated using the equations of Prescott and Hutton (1994). Based on in-situ samples, a value of 10 ± 5% water content was used in age calculations.

We report here 53 new OSL dates. All OSL dates are presented with one-sigma uncertainties. Where multiple dates were obtained for a given terrace or moraine, we determine a weighted mean age in which weights are based on the uncertainty associated with each age determination. We refer to these weighted mean ages as "mean ages."

We used ^{14}C dating for three samples of charcoal found in soil pits in terrace deposits. These samples were analyzed using AMS techniques at the University of Arizona. The ^{14}C dates were converted to calibrated ages to correct for the effects of fluctuations in the $^{14}C/^{12}C$ ratio in the atmosphere. One of the ^{14}C dates was calibrated using the program CALIB 5.0, according to the technique described in Stuiver and Reimer (1993), Stuiver et al. (1998), and Reimer et al. (2004). Two samples are beyond the range of calibration.

We also used soil development indices to correlate principal terrace levels and to evaluate the dates determined by OSL and radiocarbon. Soils were described according to standard methods and nomenclature of the U.S. Soil Survey Staff (1993). Sample analyses were conducted at the Desert Research Institute's Soil Characterization and Quaternary Pedology Laboratory. Time-related changes in soil morphology were analyzed using a well-tested soil development index (SDI; Harden, 1982; Harden and Taylor, 1983; McDonald et al., 1996). Calculation of SDI values is based on a conversion of soil morphology into numerical data to enable a quantitative comparison of the degree of soil development. Points are assigned to each property based on the difference between the described soil property and the parent material. Index values were calculated using morphologic properties of rubification, texture, structure, dry consistence, moist consistence, secondary carbonates, lightening, and argillans. The primary value produced by the SDI is the Profile Development Index (PDI) value which reflects the overall degree of soil development. The PDI values provide a means of comparison among soils within a given sequence or area and can be used to develop a soil chronofunction. We plot PDI values using mean age estimates for dated terraces to evaluate both radiometric age estimates and correlations of terrace stratigraphy between the Cinca and Gállego Rivers. The SDI has proven useful for providing correlations and calibrated age estimates for undated surfaces.

4. Distribution and chronology of glacial and fluvial morphosedimentary records

4.1. Cinca River valley

We focus on five Pleistocene terraces preserved along the Cinca River (Sancho, 1988), numbered Qt5, Qt6, Qt7, Qt8, and Qt9 from oldest to youngest, and on outcrops of glacial tills near the headwaters of the Cinca (Fig. 2a). Table I shows the results from OSL dating.

Terraces Qt5 and Qt6 are well-developed in the lower, Ebro basin reach of the river (Fig. 2e). Between Monzon and Fraga (Fig. 1), they are 60-80 m above the active channel (Fig. 2a and e). We obtained two dates (Table I) for Qt5 (171 ± 22 ka and 180 ± 12 ka), giving a weighted mean age of 178 ± 21 ka, and one date for Qt6 (97 ± 16 ka) (Table I). In additon, a single sample of eolian silt (loess) on top of fluvial gravels of the Qt5 gave an age of 20 ± 3 ka.

The relative degree of soil development is consistent with the stratigraphic separation between the Qt5 and Qt6 terraces and the age estimates (Fig. 3; Table III). The Qt5 soils at Belver (RCT6-1, RCT6-2, RCT6-3) have PDI values that range from 45.1 to 59.9, and have well developed Bk and Bkm horizons with stage III^+ to IV^+ carbonate morphology. Only one soil was described on the Qt6 surface at Belver (RCT5-1). This soil is weaker in development relative to the soils on the Qt5, having a PDI of 43.0, a well developed Btk horizon, and strong stage III^+ carbonate morphology. The difference in soil development corroborates the younger age of the Qt6 terrace, although we have only one observation on this terrace for comparison with other terraces.

The Cinca Qt7 terrace (Fig. 2c, d and e) is prominent in the landscape (~4 km wide along the Ebro basin reach of the river and 35-50 m above the active channel) and can be traced along 140 km of the river's length. Fourteen OSL dates were obtained on this terrace (Table I). Two samples from overbank sands on Qt7 terrace remnants at Alfántega and El Grado (Fig. 2a) gave dates of 52 ± 11 ka and 54 ± 9 ka and likely correspond to large floods during formation of the next younger terrace Qt8 (see below). However, they overlap other dates in this group within uncertainties. One date of 28 ± 5 ka came from a sand lens riddled with insect burrows and likely resulted from light exposure due to bioturbation. Six samples constitute a tightly grouped set of dates with a weighted mean age of 61 ± 4 ka. Finally, five dates from this terrace are significantly older than the cluster of dates that fall between 56 and 64 ka; these five dates fall into two groups with weighted mean ages of 126 ± 11 ka and 86 ± 12 ka respectively. One of these dates comes from an isolated terrace remnant at Ligüerre de Cinca (Table I) that has an elevation above the active channel similar to Qt7 remnants upstream and downstream. However, without further geochronologic data, we cannot rule out the possibility that this is a remnant of a terrace older than Qt7. We therefore interpret all these older dates as coming from remnants of older terraces incorporated into Qt7.

Five soils described on Qt7 terraces at Monzón, Albalate, and Almudáfar (RCTM4-1, RCTM4-2, RCT4-1, RCT4-2, RCTZ4-1) have PDI values ranging from 27.0 to 33.3 and with moderately- to well-developed Btk horizons and stage II to weak stage III carbonate morphology (Fig. 3; Table III). The soils developed on the Qt7 terraces are noticeably less developed than soils on the older Qt5 and Qt6 terraces, indicating that the soils on the Qt7 terraces must be considerably younger than the best age of 97 ± 16 ka for the Qt 6 terrace. Moreover, the five PDI values for the soils form a tight cluster around the best fit line, generally supporting an age of ~61 ka for the Qt7 surface. We note that the soil pits at Albalate and Almudáfar were the source of four OSL dates, three of which fall in the range 56-65 ka.

The Cinca Qt8 terrace is not as extensively preserved as the Qt7. It crops out only along the lower 35 km of the river, where it is ~2-3 km wide and sits about 20 m above the river (Fig. 2e). We have obtained six OSL dates (Table I) on Qt8 deposits, four of which are from the same outcrop at Fraga (Fig. 2a). Three of these latter dates range from 39 ± 5 ka to 50 ± 3 ka and overlap within uncertainties; the fourth is considerably older (79 ± 6 ka) and perhaps reflects incorporation of an older terrace remnant, although there is no observable geomorphic reason why this sample might be older than the rest. The six dates on Qt8 give a best age of 51 ± 4 ka. Disregarding the outlier gives an age of 47 ± 4 ka, which is the same within uncertainties.

Two soils were described on the Qt8 terrace at Albalate (RCT3-1, RCT3-2) with PDI values of 24.7 and 23.2 (Fig. 3; Table III). These soils have moderately developed Btk horizons with stage I^+ carbonate morphology. The soils on the Qt8 are less developed relative to the soils on the Qt7 terrace, supporting the OSL age of 47 ± 4 ka for the Qt8; however, the PDI values of the two soils fall below the the best fit line, suggesting that these soils may be younger than the best age estimate for the Qt8.

The Cinca Qt9 (Fig. 2e) terrace sits about 6-10 m above the active channel of the Cinca River. It is generally co-extensive with the Qt7 and traceable along ~140 km of the river's total length. The Qt9 is also approximately co-extensive with the Qt8, where the latter is preserved, and much the same width (~2 km wide). We have obtained eight OSL dates (Table I) on sand lenses within gravels of the Qt9 terrace along the Ebro basin reach, achieving good repeatability on three samples from Castejón del Puente and two samples from Chalamera (Fig. 2a). All dates are well grouped, ranging from 9 to 14 ka. The weighted mean age for these deposits is 11 ± 1 ka.

This age is corroborated by soils on the Qt9 terrace at Castejón del Puente and Albalate (RCT2-1, RCTM-1). The two soils have PDI values of 14.7 and 18.1 (Fig. 3; Table III) and moderately developed Bw and Bk horizons with stage I-II carbonate morphology. The PDI values of these soils bracket the best fit line, supporting an age of about 11 ka for the Qt9 terrace. OSL dates from Castejón del Puente and Albalate come from the soil pits.

At Ainsa (Fig. 2a), we obtained two ^{14}C dates from the base of a thick sequence of overbank sand on top of terrace gravels close to the elevation of the active channel (Table II). These dates, 18.6 cal ka BP and 22.1 ± 0.2 ka radiocarbon BP, constrain the gravels beneath to be at least that old and demonstrate the existence of important floods during the Last Glacial Maximum.

In addition, near the headwaters of the Cinca at Salinas and San Marcial (~ 25 km from the headwaters; Fig. 2a), we mapped and dated glacial and fluvioglacial deposits (Fig. 2b). The lack of interfingering relationships between these deposits and terrace remnants in the area makes direct correlation difficult to confirm. Four OSL dates on these deposits range from 46 ± 4 ka to 76 ± 13 ka. The oldest one (San Marcial) clearly corresponds to a fluvioglacial deposit with terrace morphology located 1 km to the south. The one young date among these four seems anomalous and may pertain to a later phase of glaciation; the outcrop was deformed by ice pushing (Fig. 2b), which may have mixed superposed deposits from two phases of glaciation. The weighted mean age for the three older dates is 64 ± 11 ka, which is similar to the Qt7 age (61 ± 4 ka). Based on OSL dates and geomorphic position, we correlate these glacial deposits with the Qt7 and propose that the Qt7 terrace deposits are glacial outwash.

4.2. Gállego River valley

In the valley of the Gállego River, the fluvial terrace sequence is more complicated than that of the Cinca. Controlled by Pyrenean structure, the trace of the river undergoes abrupt changes in direction (Fig. 4a). Along the Pyrenean reach of the river, the degree of incision of the Gállego River is small, whereas once the river enters the Ebro basin at Murillo (Fig. 4a and e) incision is substantially greater, thereby making correlation of terrace remnants by elevation alone impractical. Nevertheless, using OSL dates and soil development we have differentiated and mapped a system of three terrace levels along both reaches that we call "upper," "middle," and "lower." In addition, a well-preserved sequence of moraines lies along the Pyrenean reach of the Gállego valley (Fig. 4b). Table I shows the results from OSL dating.

The upper terrace is represented by remnants preserved along both reaches. In the Ebro basin, this terrace is found 72 m and 46 m above the active channel at Concilio and Gurrea de Gállego respectively (Fig. 4a). We have dated three samples (156 ± 22 ka, 148 ± 8 ka, and 140 ± 18 ka), obtaining similar ages in both localities. Upstream, near Sabiñánigo (Fig. 4a and b), fluvioglacial remnants of this terrace level are located 51 m above the active channel. Included in these deposits are glacially striated boulders more than 70 cm in diameter. We dated four samples from the upper terrace at Sabiñánigo (84 ± 9 ka, 99 ± 11 ka, 155 ± 24 ka, and 156 ± 10 ka).

Soil development indices show that the older ages are more reasonable for upper terrace soils (RGAT7-1, RGAT7-2), with the overall degree of soil development similar to soils on the ~178 ka Cinca River Qt5 terrace (Fig. 3; Table III). Upper terrace soils have well-developed Bt to Bkm horizons; however, the degree of carbonate morphology is weaker relative to similar age soils on the Cinca because the soils on the Gállego upper terrace have formed at higher elevations and under a more humid climate, factors that favor developed Bt horizons and limit develoment of carbonate morphology. As a consequence, the best age for this terrace is the 151 ± 11 ka weighted mean of five dates from Concilio, Gurrea, and Sabiñánigo, excluding the two anomalously young ages from Sabiñánigo.

The middle terrace is well preserved along the Pyrenean reach of the Gállego and shows clear evidence of fluvioglacial activity. We observed several intervals of large diameter boulders (up to 110 cm), in particular at the gravel pit at Hostal de Ipiés (Fig. 4d). Between Sabiñánigo and La Peña (Fig. 4a), the height of this terrace above the active channel is 11-17 m, although in the gravel pit at Ipiés the strath is at the same elevation as the active channel. Two dates from Hostal de Ipiés (66 ± 4 ka) and Llano de Yeste (74 ± 10 ka) agree within uncertainty. From a soil pit at Sabiñanigo, we dated two more fluvioglacial samples, one of which gave a date (69 ± 8 ka) that agrees well with dates from Hostal de Ipiés and Llano de Yeste. The other date from this soil pit (103 ± 7 ka) comes from fine sand with abundant silt-sized matrix on top of the Gállego gravels, suggesting turbid water conditions during deposition. This sample may have been incompletely zeroed. The weighted mean age for these fluvioglacial deposits, excluding the older date, is 68 ± 7 ka. The two soils described on the middle terrace at Sabiñánigo and Llano de Yeste (RGAT9-1, RGLA-9-1) are very similar in development to the soils developed on the Qt7 terraces of the Cinca River (Fig. 3; Table III), supporting OSL age estimates for the middle terrace of the Gállego and stratigraphic correlation with the Cinca Qt7.

The lower terrace is more or less continuous along the length of the Gállego valley. The strath height above the active channel is <5 m in the valley of La Peña (Fig. 4a), but increases at Murillo to 45 m and decreases from there downstream to 35 m at Biscarrués. We have dated three samples from La Peña and Biscarrués (32 ± 4 ka and 45 ± 3 ka respectively). The date from

La Peña could be too young because this outcrop shows abundant insect burrows and may have been modified by bioturbation. A soil described on the lower terrace at Marracos (Fig. 4a;) has a PDI of 22.3, moderately-developed Bwk and Bk horizons, and a stage II carbonate morphology similar in development to a soil developed on the Qt8 terrace of the Cinca River (RGAT2-1; Fig. 3; Table III). This supports the age estimate for the lower terrace of the Gállego at Biscarrués and stratigraphic correlation with the Qt8 terrace of the Río Cinca, although more data are needed to confirm this.

Near the headwaters of the Gállego, we mapped and dated two moraine deposits (Fig. 4b), one at Senegüe that retains its arcuate terminal moraine form (Fig. 4c) and one at Aurin that is degraded and retains none of its original geomorphic form. The two samples from Senegüe are from laminated sands and silts that overlie till of the moraine. The dates are quite consistent (36 ± 3 ka and 36 ± 2 ka) and give a weighted mean age of 36 ± 3 ka. One sample from Aurin, dated at 85 ± 5 ka, is from laminated sands within a till sequence. A second sample from Aurin gave a date of 38 ± 4 ka. Owing to the moraine's geomorphic position downstream of the Senegüé moraine, we consider the older date more reasonable.

The soil on the Aurin moraine (AMOR-1), with a PDI of 21.6, is clearly much better developed relative to the soil on the Senegüe moraine (SMOR-1), with a PDI of 11.3, indicating that the Aurin moraine is older (Table III). This is the common way to use soils on moraines (Birkeland, 1999). As moraines in many cases are dynamic features with episodic surface erosion, soils should be viewed as minimum relative age indicators.

5. Discussion

5.1. Reliability of methods

The reliability of OSL dating of the terrace deposits is confirmed by the excellent agreement among the eight Qt9 dates. Some dispersion in the OSL dates is apparent in the older terrace deposits. This is in some cases due to bioturbation, but may also reflect incorporation of older terrace remnants during reworking by floods. Nonetheless, the dates obtained from Qt7 are so well grouped that the weighted mean for all dates (64 ± 3 ka), including outliers, is the same as the weighted mean calculated from the six dates that fit best with geomorphic relations and soil development (61 ± 4 ka).

There is also a high degree of correspondence among OSL dates and time-related changes in degree of soil development for correlated terrace remnants. Soil PDIs provide an important means of confirming OSL dates, highlighting the utility and importance of using more than one technique to date glacial and fluvial materials, where possible. The soils best denote the age of surface stability and will not always reflect the age of deposition, however. It is possible, indeed likely, that deposition will occur over many years before the fluvial system changes to one of channel incision and yields stabilized soil-terrace surfaces.

5.2. Regional morphosedimentary glacial sequence

In the valley of the Gállego River, glacial and fluvioglacial sediments are more abundant and better preserved than in the Cinca valley. We have dated glacial sediments (Fig. 5) on the Gállego at 85 ± 5 ka and 36 ± 3 ka. An intermediate cold stage is represented by glacial sediments near the Cinca headwaters dated at 64 ± 11 ka. Eolian silt (loess) on the Cinca provides evidence of a cold stage at 20 ± 3 ka (Fig. 5) as loess acumulation is generally associated with Pleistocene glaciations (Liu et al., 1993). Correlated glacial and loess deposits have also been identified in Central Europe (Bradley, 1995).

From our data, we propose a regional, multi-phase model of glaciation, with single or multiple events within the periods 90-80 ka, 75-52 ka, 39-32 ka, and 22-17 ka. Our results confirm that the maximum extent of glacial ice in the southern Pyrenees during the last glacial occurred at 64 ± 11 ka, well prior to the LGM (García-Ruiz et al., 2003; Sancho et al., 2003). Fluvial discharge from melting LGM glaciers was small, as evidenced by the scarcity of corresponding terrace deposits. This is consistent with the well established view that glaciers during the LGM were restricted to the headwaters of river drainages in the Central Pyrenees (García-Ruiz et al., 2003; Pallás et al., 2006). During marine isotope stage 2 (MIS 2), loess accumulation (dated at 20 ± 3 ka) took place in areas of the Ebro basin adjacent to the Cinca and Gállego Rivers, locally covering some previous terrace surfaces. By contrast with the rest of the Pyrenees, the maximum ice advance in the eastern Pyrenees occurred late, during MIS 2 (Delmas et al., 2008).

In general, our chronology of glacial events in the Pyrenees bolsters previous models derived from geomorphic and stratigraphic relations in other areas of the Pyrenees (Vilaplana, 1983; Bordonau, 1992; García-Ruiz and Martí-Bono, 1994; Chueca et al., 1998; Serrano, 1998) while demonstrating via OSL dating and soils geomorphology that the southern European glacial maximum hypothesized by previous authors, well prior to the LGM, is essentially correct. Asynchroneity of glaciation in southern Europe with respect to northern Europe has also been documented in the Cantabrian Mountains of Spain (Jiménez and Farias, 2002), the French Pyrenees (Hérail et al., 1986; Andrieu et al., 1988; Jalut et al., 1992), the French Vosges (Seret et al., 1990), the Swiss Alps (Chapron, 1999), the Italian Apennines (Giraudi and Frezzotti, 1997; Kotarba et al., 2001), and the Pindus Mountains in Greece (Woodward et al., 2004).

5.3. Regional morphosedimentary fluvial sequence

The robust correlation among terraces on the two rivers allows us to construct a regional morphogenetic model of glacial outwash and terrace development at 178 ± 21 ka to 151 ± 11 ka, ca. 97 ka, 68 ± 7 ka to 61 ± 4 ka, 47 ± 4 ka to 45 ± 3 ka, and 11 ± 1 ka (Fig. 5). In additon, evidence of fluvial activity at 126 ± 11 ka, 86 ± 12 ka, and ca. 22-18 ka has been noted, but no mapped terrace remnants correspond to these deposits.

For the rest of the Pyrenees and Ebro basin, chronologic data on terraces are almost non-existent, and more data are required to thoroughly test our regional model. Nevertheless, some comparisons can be made with previously published data. In the central Ebro basin, Luzón et al. (2008) obtained four OSL ages grouped around 78-73 ka and 58-50 ka from Ebro River terraces affected by synsedimentary karstic subsidence. One of the best developed terraces in the Cinca-Gállego system (68 ± 7 ka to 61 ± 4 ka) overlaps the ages of the Ebro terraces within uncertainties, suggesting a link not only between periods of alluviation but also between periods of glacial outwash and formation of karst topography. On the southern side of the Ebro basin (Guadalope River and tributaries), Fuller et al. (1998) differentiated a series of fluvial aggradational episodes (based on infrared stimulated luminescence dating), which they associated, in most cases, with marine isotope stages and Heinrich events (H) as follows: MIS 6, MIS 5e, transition MIS 5e-5d, MIS 5b, MIS 3 (including one event centered on H4), and MIS 2 (with an event centered on H1). These aggradational episodes are thought to coincide with stadials (Fuller et al., 1998), although these rivers were not glaciated in their headwaters. Some, but not all, of these aggradational events can be correlated with the Cinca and Gállego chronology (MIS 6, MIS 5e, MIS 5b, H4, and H1) and with other records across the Mediterranean basin (Macklin et al., 2002).

Other important Iberian rivers (Duero, Tajo and Guadalquivir; Pérez-González et al., 1994; Pérez-González et al., 2004; Díaz del Olmo et al., 1989) have extensive multi-stage terrace sequences constrained by paleontological, paleomagnetic, and archaeological data. However, these data do not permit definitive correlation with the terrace systems of the Cinca and Gállego Rivers. Thorndycraft and Benito (2006) identified a period of greater frequency of large magnitude floods at 12-10 ka on the Tajo River, which coincides with a cold climatic phase. This event could correlate with the Qt9 on the Cinca River.

As alluvial aggradation in the southern Iberian Peninsula is partially controlled by tectonic activity (Harvey and Wells, 1987; Harvey et al., 1995; Candy et al., 2004), we hesitate to make correlations with those chronologies.

5.4. Correlation at global scale

High resolution proxy climate data for the last 250 kyr from the Alborán Sea (southwestern Mediterranean basin; Martrat et al., 2004) suggest that periods of alluviation registered on the Cinca and Gállego may coincide with cold phases in a context of highly variable climate marked by abrupt climate changes, although an exact fit for all alluvial stages is not apparent. Stages of terrace development appear to be associated with stadials, marked by the lowest values of $\delta^{18}O$ in G. bulloides, lowest sea surface temperatures, and highest percentages of Tenaghi Philippon woody taxa (Martrat et al., 2004).

At the global scale, our chronology of meltwater discharge events and terrace development coincides with maxima in insolation at 65° N during the summer solstice (Berger and Loutre, 1991) (Fig. 5b). The chronology of terrace development also corresponds reasonably well with the SPECMAP standard $\delta^{18}O$ isotopic curve obtained from deep sea sediments (Martinson et al., 1987) (Fig. 5c). There is a general correlation between alluvial events and MIS

6, 5e, transition 5c-5b, 5a, transition 4-3, 3, and transition 2-1 (Fig. 5d; Martinson et al., 1987). From the curve that relates ice-rafted debris (IRD; McManus et al. 1999) in North Atlantic sediments to Heinrich events (Bond et al., 1992, 1993), we see a coincidence between some peaks of detrital discharge in the ocean and stages of alluviation in the Cinca and Gállego River valleys (~128 ka; H6; ~60 ka; H5; H1, and the Younger Dryas at ~12 ka; Fig. 5e). Fluvial aggradation appears to respond to the same climate signals as does marine sedimentation. Solar forcing drives melting of sea ice and glacial ice, causing freshwater pulses that affect thermohaline circulation in the North Atlantic.

In the southern Pyrenees, the glacial stage at 64 ± 11 ka represents the maximum extent of ice during the Late Pleistocene in the southern Pyrenees and resulted in massive fresh water discharge on both the Cinca and Gállego Rivers. What was different during stage 4? The answer may lie in the direction and intensity of storm tracks in the North Atlantic. Climate during stage 4 is known to have been warmer than stage 2, but perhaps it was stormier, delivering more precipitation to Iberia than during stage 2.

Global circulation models have demonstrated that Iberian rainfall is mainly influenced by anomalies in atmospheric circulation in the North Atlantic, not by regional or remote sea surface temperature anomalies (Zorita et al., 1992). A close relationship exists between the North Atlantic Oscillation and rainfall in northwest Africa, Iberia, and other parts of Western Europe (Meehl and van Loon, 1979; Zorita et al., 1992; Hurrell, 1995). The severity of Pyrenean glaciations might therefore be connected to the intensity of atmospheric circulation (Florineth and Schlüchter, 2000). During MIS 4, the North Atlantic polar front occupied an intermediate latitudinal position (Ruddiman and McIntyre, 1977), resulting in transfer of heat and moisture from warm subtropical water to the atmosphere in the path of the prevailing westerlies that bring storm tracks across Iberia. During the LGM, the jet stream was deflected far south by the extreme zonal position of the North Atlantic polar front, resulting in high lake levels in the Tibesti Mountains of North Africa (Maley, 2000) and leaving Iberia dry. The extent of ice sheets in the Barents and Kara Seas (determined by distribution of IRD on the continental shelf) also appears coupled to the influence of Atlantic water and therefore moisture supply (Siegert & Dowdeswell, 2004). MIS 4 was marked by continuous Atlantic water inflow and eastward penetration of moisture-bearing storms, resulting in major ice sheet buildup in the Kara Sea (Knies et al., 2001). MIS 2, on the other hand, was a less intense glaciation, with no ice in the Kara Sea. The magnitude of the MIS 4 glaciation in the Pyrenees may have been driven by oceanic moisture and sea level feedbacks, amplifying the precessional insolation minimum that occurred at that time (Ruddiman and McIntyre, 1981).

6. Conclusions

The robust chronological correlation of glacial, fluvioglacial, and fluvial deposits along the Cinca and Gállego Rivers (Pyrenees and Ebro basin, northeastern Spain), based on consistency between geomorphic field relations, chronologic data from optically stimulated luminescence dating, and soil development, allows us to draw the following conclusions:

1. We have combined radiometric dating results with time-related trends in soil development to make reasonable age interpretations that support the idea that fluvial terraces [Cinca Qt5 (Gállego upper), Cinca Qt7 (Gállego middle), Cinca Qt8 (Gállego lower)] are regionally correlative.

2. We have developed a regional morphogenetic glacial sequence consisting of periods of glacial stability at 85 ± 5 ka, 64 ± 11 ka, 36 ± 3 ka, and 20 ± 3 ka and periods of elevated fluvial activity with development of extensive terraces at 178 ± 21 ka to 151 ± 11 ka, ca. 97 ka, 68 ± 7

ka to 61 ± 4 ka, 47 ± 4 ka to 45 ± 3 ka, and 11 ± 1 ka. In additon, equivocal evidence of alluviation at 126 ± 11 ka, 86 ± 12 ka, and ca. 22-18 ka exists within terrace deposits but not associated with mappable terrace remnants.

3. During the Late Pleistocene in northeastern Spain, the most extensive morphosedimentary glacial (64 ± 11 ka) and associated fluvial deposits (68 ± 7 ka to 61 ± 4 ka) accumulated during marine isotope stage 4 and Heinrich event 6. The maximum in glacial and fluvial activity does not coincide with the Last Glacial Maximum owing, probably, to predominantly arid conditions during the LGM on the Iberian Peninsula linked to anomalies in atmospheric circulation in the North Atlantic.

4. Large glacial meltwater discharges were involved in the formation of the terraces. We see a strong correlation between phases of fluvial aggradation and terrace development and periods of maximum insolation in the northern hemisphere, ice rafting events in the North Atlantic, and patterns of atmospheric circulation in the North Atlantic. The glacial systems and the associated fluvial dynamic during the Late Pleistocene in northern Iberia seem sensitive to solar forcing as well as North Atlantic oceanic and atmospheric circulation.

7. Acknowledgements

This work was funded by grants from the National Geographic Society, the National Science Foundation (EAR-0088714), the Spanish Ministry of Education, and a Fulbright Senior Scholar grant to the first author. We thank the Institute of Geophysics and Planetary Physics and Laboratory Directed Research and Development (LDRD) at Los Alamos National Laboratory for additional funding. Desert Research Institute and the Departamento de Geografía y Ordenación del Territorio at the University of Zaragoza provided GPS equipment. We thank Erica Bigio for assistance in the field, Marta Lopez for GIS cartography, and Martha Ros for logistical support.

8. References

Andrieu, V., Hubschman, J., Jalut, G., Herail, G., 1988. Chronologie de la deglaciation des Pyrénées françaises. Dynamique de sedimentation et contenu pollinique des paléolacs: application à l'interpretation du retrait glaciare. Bull. Assoc. Française Etude Quat. 2/3, 55-67.

Benito, G., 1989. Geomorfología de la Cuenca Baja del río Gállego. Zaragoza, Spain, PdD dissertation, Universidad de Zaragoza. 764 p.

Benito, G., Pérez-González, A., Gutiérrez, F., Machado, M.J., 1998. River response to Quaternary large-scale subsidence due to evaporite solution (Gállego River, Ebro Basin, Spain). Geomorphology 22, 243-263.

Berger, A., Loutre, M.F., 1991. Insolation values for the climate of the last 10 million years. Quat. Sci. Rev. 10, 297-317.

Birkeland, P.W., 1999. Soils and Geomorphology. Oxford University Press. New York. 430 p.

Bond, G., Broecker, W., Johnsen, S., McManus, J., Labeyrie, L., Jouzel, J., Bonani, G., 1993. Correlations between climate records from North Atlantic sediments and Greenland ice. Nature 365, 143-147.

Bond, G., Heinrich, H., Broecker, W., Labeyrie, L., McManus, J., Andrews, J., Huon, S. Jantschick, R., Clausen, S., Simet, C., Tedesco, K., Klas, M., Bonani, G., Ivy, S., 1992. Evidence for massive discharges of icebergs into the North Atlantic Ocean during the last glacial period. Nature 360, 245-249.

Bordonau, J., 1992. Els complexes glàcio-lacustres relacionats amb el darrer cicle glacial als Pirineus. Geoforma Ediciones. Logroño, Spain. 251 p.

Bout-Roumazeilles, V., Combourieu Nebout, N., Peyron, O., Cortijo, E., Landais, A., Masson-Delmotte, V., 2007. Connection between South Mediterranean climate and North African atmospheric circulation during the last 50,000 yr BP North Atlantic cold events. Quat. Sci. Rev. 26, 3197-3215.

Bowen, D.Q., Richmond, G.M., Fullerton, D.S., Šibrava, V., Fulton, R.J., Velichko, A.A., 1986. Correlation of Quaternary glaciations in the northern hemisphere. Quat. Sci. Rev. 5, 509-510.

Bradley, R., 1995. Paleoclimatology: reconstructing climates of the Quaternary. International Geophysics Series 64. Academic Press. San Diego, CA. 613 p.

Bridgland, D. Westaway, R., 2007. Climatically controlled river terrace staircases: A worldwide Quaternary phenomenon. Geomorphology. doi:10.1016/j.geomorph.2006.12.032.

Broecker, W.S., 1994. Massive iceberg discharges as triggers for global climate change. Nature. 372, 421-424.

Cacho, I., Grimalt, J.O., Sierro, F.J., Shackleton, N., Canals, M., 2000. Evidence for enhanced Mediterranean thermohaline circulation during climatic coolings. Earth Planet. Sci. Lett. 183, 417–429.

Candy, I., Black, S., Sellwood, B.W., 2004. Interpreting the response of a dryland river system to Late Quaternary climate change. Quat. Sci. Rev. 23, 2513-2523.

Chapron, E., 1999. Contrôle climatique et sismo-tectonique de la sédimentation lacustre dans l'Avant-Pays Alpin (Lac du Bourget) durant le Quaternaire récent. Géologie Alpine Memoire HS 30. Université Joseph Fournier, Grenoble. 216 p.

Chueca, J., Peña, J.L., Lampre, F., García-Ruiz, J.M., Martí-Bono, C., 1998. Los glaciares del Pirineo aragonés: estudio de su evolución y extensión actual. Departamento de Geografía y Ordenación del Territorio. Universidad de Zaragoza, Zaragoza, Spain. 104 p.

Delmas, M., Gunnell, Y., Braucher, R., Calvet, M., Bourlès, D., 2008. Exposure age chronology of the last glaciation in the eastern Pyrenees. Quat. Res. 69, 231-241.

Díaz del Olmo, F., Vallespí, E., Baena, R., Recio, J.M., 1989. Terrazas pleistocenas del Guadalquivir occidental: geomorfología, suelos, paleosuelos y secuencia cultural. AEQUA Monografías 1, 33-42.

Florineth, D., Schlüchter, C., 2000. Alpine Evidence for Atmospheric Circulation Patterns in Europe during the Last Glacial Maximum. Quat. Res. 54, 295-308.

Fuller, I.C., Macklin, M.G., Lewin, J., Passmore, D.G., Wintle, A.G., 1998. River response to high-frequency climate oscillations in southern Europe over the past 200 k.y. Geology 26, 275-278.

García-Ruiz, J.M., Martí-Bono, C., 1994. Rasgos fundamentales del galcairismo cuaternario en el Pirineo aragonés. In: Martí-Bono, C., García-Ruiz, J.M. (Eds.), El glaciarismo surpirenaico: nuevas aportaciones. Geoforma Ediciones, Logroño, Spain, pp. 17-35.

García-Ruiz, J. M., Valero-Garcés, B. L., Martí-Bono, C., González-Sampériz, P., 2003. Asynchroneity of maximum glacier advances in the central Spanish Pyrenees. J. Quat. Sci. 18, 61-72.

Gile, L.H., Hawley, J.H., Grossman, R.B., 1981. Soils and Geomorphology in the Basin and Range Area of Southern New Mexico - Guidebook to the Desert Project. Memoir 39: New Mexico Bureau of Mines and Mineral Resources, Socorro, NM.

Giraudi, C., Frezzotti, M., 1997. Late Pleistocene glacial events in the Central Apennines, Italy. Quat. Res. 48, 280-290.

Harden, J.W., 1982. A quantitative index of soil development from field descriptions: examples from a soil chronosequence in central California. Geoderma 28, 1-28.

Harden, J.W., Taylor, E.M., 1983. A quantitative comparison of soil development in four climatic regimes. Quat. Res. 20, 342-359.

Harvey, A.M., Wells, S.G., 1987. Response of Quaternary fluvial systems to differential epeirogenic uplift: Aguas and Feos river systems, southeast Spain. Geology 15, 689-693.

Harvey, A.M., Miller, S.Y., Wells, S.G., 1995. Quaternary soil and river terrace sequences in the Aguas-Feos river systems: Sorbas basin, southeast Spain. In: Lewin, J., Macklin, M.G., Woodward, J.C. (Eds.), Mediterranean Quaternary River Environments. A.A. Balkema, Lisse, The Netherlands. pp. 263-281.

Hérail, G., Hubschman, J., Jalut, G., 1986. Quaternary glaciation in the French Pyrenees. Quat. Sci. Rev. 5, 397-402.

Hughes, P.D., Woodward, J.C., Gibbard, P.L., 2006a. Quaternary glacial history of the Mediterranean mountains. Prog. Phys. Geog. 30, 334-364.

Hughes, P.D., Woodward, J.C., Gibbard, P.L., 2006b. Late Pleistocene glaciers and climate in the Mediterranean. Global Planet. Change 50, 83-98.

Hurrell J.W., 1995. Decadal trends in the north-Atlantic oscillation – regional temperatures and precipitation. Science 269, 676-679.

Jalut, G., Monserrat, J., Fontunge, M., Delibrias, G., Vilaplana J., Juliá R., 1992. Glacial to interglacial vegetation changes in the northern and southern Pyrenees: deglaciation, vegetation cover and chronology. Quat. Sci. Rev. 11, 449-480.

Jiménez, M., Farias, P., 2002. New radiometric and geomorphologic evidences of a last glacial maximum older than 18 ka in SW European mountains: the example of Redes Natural Park (Cantabrian Mountains, NW Spain). Geodinámica Acta 15, 93-101.

Knies J., Kleiber H.-P., Matthiessen J., Mueller C., Nowaczyk N.R., 2001. Marine ice-rafted debris records constrain maximum extent of Saalian and Weichselian ice-sheets along the northern Eurasian margin. Global Planet. Change 31, 45-64.

Kotarba, A., Hercman, H., Dramis, F., 2001. On the age of Campo Imperatore glaciations, Gran Sasso Massif, Central Italy. Geograf. Fís. Dinám. Quat. 24, 65-69.

Liu, T., Ding, Z., Yu, Z., Rutter, N., 1993. Susceptibility time series of the Baoji section and the bearings on paleoclimatic periodicities in the last 2.5 Ma. Quat. Int. 17, 33-38.

Luzón, A., Pérez, A., Soriano, M.A., Pocoví, A., 2008. Sedimentary record of Pleistocene paleodoline evolution in the Ebro basin (NE Spain). Sediment. Geol. 205, 1-13.

Macklin, M.G., Fuller, I.C., Lewin, J., Maas, G.S., Passmore, D.G., Rose, J., Woodward, J.C., Black, S., Hamlin, R.H.B., Rowan, J.S., 2002. Correlation of fluvial sequences in the Mediterranean basin over the last 200 ka and their relationship to climate change. Quat. Sci. Rev. 21, 1633-1641.

Maley J., 2000. Last Glacial Maximum lacustrine and fluviatile formations in the Tibesti and other Saharan mountains, and large-scale climatic teleconnections linked to the activity of the Subtropical Jet Stream. Global Planet. Change 26, 121-136.

Martinson, D.G., Pisias, N., Hays, J.D., Imbrie, J., Moore, T.C., Shackleton, N.J., 1987. Age dating and the orbital theory pf the Ice Ages: development of a high resolution 0 to 300,000-year chronostratigraphy. Quat. Res. 27, 1-29.

Martrat, B., Grimalt, J.O., López-Martínez, C., Cacho, I., Sierro, F.J., Flores, J.A., Zahn, R., Canals, M., Curtis, J.H., Hodell, D.A., 2004. Abrupt temperature changes in the Western Mediterranean over the past 250,000 years. Science 306, 1762-1765.

McDonald, E.V., Reneau, S.L., Gardner, J.N., 1996. Soil-forming processes on the Pajarito Plateau: Investigation of a soil chronosequence in Rendija Canyon. In: Goff, F., Kues, B.S., Rogers, M.A., McFadden, L.D., Gardner, J.N. (Eds.), New Mexico Geological Society Guidebook, 47th Conference. Socorro, New Mexico, USA, pp. 375-382.

McManus, J.F., Oppo, D.W., Cullen, J.L., 1999. 0.5 Million years of millennial-scale climate variability in the North Atlantic. Science 283, 971-975.

Meehl G.A., van Loon H., 1979. The seesaw in winter temperatures between Greenland and Northern Europe. Part III: Teleconnections with lower latitudes. Monthly Weather Review 107, 1095-1106.

Moreno, A., Cacho, I., Canals, M., Grimalt, J.O., Sánchez-Goñi, M.F., Shackleton, N., Sierro, F.J., 2005. Links between marine and atmospheric processes oscillating on a millennial time-scale. A multiproxy study of the last 50,000 yr from the Alboran Sea. Quat. Sci. Rev. 24, 1623–1636.

Murray, A.S., Wintle, A.G., 2000. Luminiscence dating of quartz using an improved single-aliquot regenerative-dose protocol. Radiat. Meas. 32, 57-73.

Pallás, R., Rodés, A., Braucher, R., Carcailler, J., Ortuño, M., Bordonau, J., Bourlés, D., Vilaplana, J.M., Masana, E., Santanach, P., 2006. Late Pleistocene and Holocene glaciation in the Pyrenees: a critical review and new evidence from ^{10}Be exposure ages, south-central Pyrenees. Quat. Sci. Rev. 25, 2937-2963.

Pérez-González, A., Martín-Serrano, A., Pol, C., 1994. Depresión del Duero. In Gutiérrez, M. (Ed.), Geomorfología de España. Editorial Rueda. Madrid, Spain, pp. 351-388.

Pérez-González, A., Silva, P.G., Roquero, E., Gallardo, J., 2004. Geomorfología fluvial y edafología del sector meridional de la cuenca de Madrid (Toledo-Madrid). In: Benito, G., Díez Herrero, A. (Eds.), Itinerarios geomorfológicos por Castilla-La Mancha. Sociedad Española de Geomorfología, Oviedo, Spain, pp. 12-48.

Prescott, J.R., Hutton, J.T., 1994. Cosmic ray contributions to dose rates for luminescence and ESR dating: large depths and long term time variations. Radiat. Meas. 23, 497-500.

Reimer, P.J., and 28 others, 2004, INTCAL04 terrestrial radiocarbon age calibration, 0-26 cal kyr BP. Radiocarbon 46, 1029-1058.

Rhodes, E.J., 1988. Methodological considerations in the optical dating of quartz. Quat. Sci. Rev. 7, 395-400.

Ruddiman, W.F., McIntyre, A., 1977. Late Quaternary surface ocean kinematics and climatic change in the high-latitude North Atlantic. J. Geophys. Res. 82, 3877-3887.

Ruddiman, W.F., McIntyre, A., 1981. Oceanic mechanisms for amplification of the 23,000-year ice-volume cycle. Science 212, 617-627.

Sánchez-Goñi, M.F., Cacho, I., Turon, J.L., Guiot, J., Sierro, F.J., Peypouquet, J.-P., Grimalt, J.O., Shackleton, N., 2002. Synchroneity between marine and terrestrial responses to millennial scale climatic variability during the last glacial period in the Mediterranean region. Clim. Dyn. 19, 95–105.

Sancho, C., 1988. Geomorfología de la cuenca baja del río Cinca. PhD thesis, University of Zaragoza. 743 p.

Sancho, C., Peña, J.L., Lewis, C., McDonald, E., Rhodes, E., 2003. Preliminary dating of glacial and fluvial deposits in the Cinca River Valley (NE Spain): chronological evidences for the Glacial Maximum in the Pyrenees? In: Ruiz, M.B., Dorado, M., Valdeolmillos, A., Gil, M.J., Bardají, T., Bustamante, I., Martínez, I. (Eds.), Quaternary climatic changes and environmental crises in the Mediterranean region. Universidad de Alcalá-Ministerio de Ciencia y Tecnología-INQUA, Alcalá de Henares, Spain, pp. 169-173. ISBN 84-699-8798-4.

Sancho, C., Peña, J.L., Lewis, C., McDonald, E., Rhodes, E., 2004. Registros fluviales y glaciares cuaternarios en las cuencas de los ríos Cinca y Gállego (Pirineos y depresión del Ebro). In: Colombo, F., Liesa, C.L., Meléndez, G., Pocoví, A., Sancho, C. Soria, A.R., (Eds.), Itinerarios Geológicos por Aragón. Sociedad Geológica de España, Geo-Guías 1. Salamanca, Spain, pp. 181-205.

Santisteban, J.I., Schulte, L., 2007. Fluvial networks of the Iberian Peninsula: a chronological framework. Quat. Sci. Rev. 26, 2738-2757.

Seret, G., Dricot, E., Wansard, G., 1990. Evidence for an early glacial maximum in the French Vosges during the last glacial cycle. Nature 346, 453-456.

Serrano, E., 1998. Geomorfología del Alto Gállego (Pirineo aragonés). Institución Fernando el Católico. Zaragoza, Spain, 501 p.

Schackleton, M.J., Opdyke, N.D., 1973. Oxygen isotope and paleomagnetic stratigraphy of equatorial Pacific core V28-238: oxygen isotope temperature and ice volumes on a 10^5 and 10^6 year scale. Quat. Res. 1, 39-55.

Siegert, M.J., Dowdeswell, J.A., 2004. Numerical reconstructions of the Eurasian ice sheet and climate during the later Weichselian. Quat. Sci. Rev 23, 1273-1283.

Stuiver, M., Reimer, P. J., 1993. Extended ^{14}C database and revised CALIB radiocarbon calibration program. Radiocarbon 35, 215-230.

Stuiver, M., Reimer, P.J., Bard, E., Beck, J.W., Burr, G.S., Hughen, K.A., Kromer, B., McCormac, F.G., v. d. Plicht, J., Spurk, M., 1998. INTCAL98 Radiocarbon age calibration 24,000 - 0 cal BP. Radiocarbon 40, 1041-1083.

Thorndycraft, V.R., Benito, G., 2006. The Holocene fluvial chronology of Spain: evidence from a newly compiled radiocarbon database. Quat. Sci. Rev. 25, 223-234.

U.S. Soil Survey Staff, 1993. Examination and description of soils. In: Soil Conservation Service. Soil survey manual. U.S. Department of Agriculture Handbook 18. Washington, D.C., USA, Chapter 3.

Vilaplana, J.M., 1983. Quaternary glacial geology of the Alta Ribagorza basin (Central Southern Pyrenees). Acta Geológica Hispánica 18, 217-233.

Woodward, J.C., Macklin, M.G., Smith, G.R., 2004. Pleistocene glaciaiton in the mountains of Greece. In: Ehlers, J. Gibbard, P.L. (Eds.), Quaternary glaciations: extent and chronology, Part I: Europe. Elsevier, Amsterdam, The Netherlands, pp. 155-173.

Zorita, E., Kharin, V., von Storch, H., 1992. The atmospheric circulation and sea surface temperature in the North Atlantic area in winter: Their interaction and relevance for Iberian precipitation. J. Clim. 5, 1097-1108.

Tables

Table I. OSL dates from moraines and terraces on the Cinca and Gállego Rivers (italic letters indicate dates which are not in agreement with geomorphological context).

Table II. ^{14}C results from Cinca River terrace deposit.

Table III. Summary of soil PDI values and B horizon development.

Figure Captions

Figure 1. Location of the study area in the northeastern Iberian Peninsula. Digital elevation model from SRTM data.

Figure 2. Glacial and fluvial deposits of the Cinca River: a) Distribution of glacial tills and fluvial terrace deposits along the Cinca valley, b) Outcrop of moraine deposits near the headwaters of the Cinca (at Salinas), c) Qt7 morphogenetic surface and related deposits at Ainsa with the Internal Pyrenees in the background, d) Qt7 terrace deposits near Albalate, with sand lens at base of outcrop used for OSL dating, e) Detailed geomorphological map of terrace sequence in the Ebro basin reach of the Cinca River.

Figure 3. Profile Development Index (PDI) values plotted with mean radiometric (OSL) age estimates for terraces along the Cinca and Gállego Rivers. Best fit line to linear regression uses soil and OSL data for both rivers. Hatched bars are PDI age ranges (one-sigma).

Figure 4. Glacial and fluvial deposits on the Gállego River: a) Distribution of glacial and fluvial deposits along the Gállego valley, b) Detailed geomorphological mapping of moraines and terraces near the headwaters of the Gállego River, c) Senegüé terminal moraine, d) Gállego middle terrace deposits near Hostal de Ipiés, showing abundant boulders, e) Gállego lower terrace at Murillo with the External Pyrenees in the background.

Figure 5. Phases of glacial and fluvial activity on the Cinca and Gállego Rivers (northern Spain) related to other paleoenvironmental records (adapted from Martrat et al., 2004): a) Weighted mean ages with uncertainties of glacial, fluvial, and eolian (loess) morphosedimentary units, b)

Insolation at 65°N during summer (Berger and Loutre, 1991), c) SPECMAP standard isotope curve (Martinson et al., 1987), d) Marine isotope stages (Martinson et al., 1987), e) Proportion of detrital lithics (ice rafted debris; McManus et al. 1999) and Heinrich ice rafting events (Bond et al., 1992, 1993) in North Atlantic marine sediments. Abbreviations: QtUp, Gállego upper terrace; QtMid, Gállego middle terrace; QtLow, Gállego lower terrace. Vertical bars show correlations of dated glacial and fluvial deposits with climate proxies (width of bars not scaled to reflect uncertainties).

Table I. OSL dates from moraines and terraces on the Cinca and Gállego Rivers.

Oxford Lab Code	Northing (m)	Easting (m)	Elevation (m)	Location	Terrace No.	Soil No.	De (Gy)	Dose rate (mGy/a)	OSL date (ka)
Cinca River									
	Fluvioglacial deposits								
X814*	4718674	271870	789	Salinas de Sin	NA		127 ± 7	2.77 ± 0.17	46 ± 4
X815*	4718674	271870	789	Salinas de Sin	NA		161 ± 13	2.60 ± 0.15	63 ± 6
X829*	4718674	271870	789	Mesón de Salinas	NA		161 ± 33	2.28 ± 0.15	71 ± 15
X831*	4718480	270710	760	San Marcial	NA		141 ± 22	1.85 ± 0.12	76 ± 13
X818	4619704^	268358	247	Belver	Qt4-loess	RCT7-3	58 ± 7	2.96 ± 0.19	20 ± 3
	Qt5 fluvial terrace								
X399	4619473	266357	217^	Belver	Qt5	RCT6-2	209 ± 7	1.16 ± 0.7	180 ± 12
X398	4618380	266866	215^	Belver	Qt5	RCT6-1	237 ± 26	1.39 ± 0.09	171 ± 22
	Qt6 fluvial terrace								
X397	4618085	266253	200	Belver	Qt6	RCT5-1	157 ± 23	1.62 ± 0.11	97 ± 16
	Qt7 fluvial terrace								
X396	4700762	265624	585^	Pueyo de Araguas	Qt7		156 ± 26	2.46 ± 0.18	63 ± 12
X1122*	4700762	265624	585^	Pueyo de Araguas	Qt8		128 ± 27	2.16 ± 0.12	59 ± 13
X395	4700762	265624	575^	Pueyo de Araguas	Qt7		84 ± 15	3.00 ± 0.21	28 ± 6
X825	4692548	268289	534	Ainsa	Qt7		241 ± 22	1.88 ± 0.12	128± 14
X824	4684406	269987	487	Ligüerre de Cinca	Qt7		161 ± 6	1.85 ± 0.12	87 ± 7
X823	4678877	270913	461	Moscarazos	Qt7		82 ± 15	1.28 ± 0.08	64 ± 13
X827	4669786	270753	404^	El Grado	Qt7		94 ± 14	1.75 ± 0.11	54 ± 9
X822	4634387	263310	247	Alfántega	Qt7		128 ± 26	2.44 ± 0.16	52 ± 11
X820	4633077	263267	243	Alfántega	Qt7		117 ± 16	1.40 ± 0.09	83 ± 13
X811*	4633077	263267	243	Alfántega	Qt7		196 ± 10	1.46 ± 0.07	134 ± 9
X197	4618846	265647	262^#	Albalate-Belver	Qt7	RCT4-1	150 ± 3	2.45 ± 0.12	61 ± 3
X199	4613809	267775	173	Almudáfar	Qt7		101 ± 5	1.80 ± 0.09	56 ± 4
X198	4613809	267775	173	Almudáfar	Qt7		118 ± 5	1.82 ± 0.10	65 ± 5
X810*	4613809	267775	173	Almudáfar	Qt7		223 ± 5	1.84 ± 0.10	121 ± 7
	Qt8 fluvial terrace								

X817	4624970^	262087	184[#]	Albalate	Qt8	RCT3-1	89 ± 10	2.26 ± 0.14	39 ± 5
X821	4614698	267127	154	Almudáfar	Qt8		83 ± 10	1.96 ± 0.13	42 ± 6
X833*	4598786	279236	112	Fraga	Qt8		117 ± 6	2.50 ± 0.16	47 ± 4
X834	*4598802*	*279195*	*109*	*Fraga*	*Qt8*		*150 ± 5*	*1.89 ± 0.13*	*79 ± 6*
X808*	4598765	278848	109	Fraga	Qt8		88 ± 4	1.75 ± 0.10	50 ± 4
X809*	4598765	278848	109	Fraga	Qt8		90 ± 2	1.79 ± 0.11	50 ± 3
	Qt9 fluvial terrace								
X828	4667581	270671	358	El Grado	Qt9		18 ± 1	1.86 ± 0.12	10 ± 1
X826*	4648906	266149	271	Castejón	Qt9		22 ± 1	1.89 ± 0.13	12 ± 1
X812*	4648906	266149	271	Castejón	Qt9		18 ± 8	1.46 ± 0.07	9 ± 4
X813*	4648906	266149	271	Castejón	Qt9		27 ± 4	1.91 ± 0.10	14 ± 2
X816	4625045^	261783	178[#]	Albalate	Qt9	RCT2-1	27 ± 2	2.15 ± 0.14	12 ± 1
X806*	4618197	263357	160	Chalamera	Qt9		23 ± 2	2.03 ± 0.11	11 ± 1
X807*	4618197	263357	160	Chalamera	Qt9		22 ± 1	1.96 ± 0.10	11 ± 1
X832	4605683	275009	117	Zaidín	Qt9		18 ± 4	1.81 ± 0.12	10 ± 2
Gallego River									
	Glacial deposits								
X1143*	4713769	718320	822	Senegüe	moraine		84 ± 7	2.35 ± 0.10	36 ± 3
X1144*	4713769	718320	822	Senegüe	moraine	SMOR-1	69 ± 2	1.94 ± 0.07	36 ± 2
*X1127**	*4711957*	*717750*	*785*	*Aurin*	*moraine*		*56 ± 6*	*1.48 ± 0.07*	*38 ± 4*
X1128*	4711957	717750	785	Aurin	moraine	AMOR-1	118 ± 4	1.39 ± 0.06	85 ± 5
	Upper terrace								
X1112*	4687422	685514	509	Concilio	upper		280 ± 36	1.80 ± 0.10	156 ± 22
X1114*	4656724	685892	360	Gurrea	upper		173 ± 4	1.17 ± 0.05	148 ± 8
X1115*	4656724	685892	360	Gurrea	upper		168 ± 20	1.20 ± 0.06	140 ± 18
	Fluvioglacial deposits								
*X1137**	*4709862*	*716641*	*801*[#]	*Sabiñanigo Alto*	*upper*	*RGA2-2*	*165 ± 16*	*1.67 ± 0.07*	*99 ± 11*
*X1138**	*4709862*	*716641*	*801*[#]	*Sabiñanigo Alto*	*upper*	*RGA3-2*	*145 ± 14*	*1.72 ± 0.08*	*84 ± 9*
X1139*	4709862	716641	801[#]	Sabiñanigo Alto	upper	RGA4-2	255 ± 38	1.64 ± 0.08	155 ± 24
X1140*	4709862	716641	801[#]	Sabiñanigo Alto	upper	RGA5-2	252 ± 12	1.61 ± 0.07	156 ± 10
	Fluvioglacial deposits								
*X1141**	*4709321*	*717174*	*770*	*Sabiñanigo*	*middle*	*RGAT7-2*	*151 ± 8*	*1.47 ± 0.07*	*103 ± 7*
X1142*	4709321	717174	770	Sabiñanigo	middle	RGAT7-2	125 ± 13	1.81 ± 0.09	69 ± 8
X1126*	4701910	712613	704	Hostal de Ipies	middle	RGIT7-1	91 ± 4	1.38 ± 0.06	66 ± 4
X1106*	4694454	690726	553[#]	Llano de Yeste	middle	RGLA9-1	104 ± 13	1.41 ± 0.05	74 ± 10
	Lower terrace								
X1116*	4694492	690682	553	La Peña	lower		40 ± 4	1.27 ± 0.05	32 ± 4
X1124*	4677559	684914	462	Biscarrués	lower		51 ± 3	1.13 ± 0.04	45 ± 3

A value of 10 ± 5% water content was assumed for all samples.
* Dose rate is based on in-situ gamma spectroscopy. For all other samples, dose rate values are calculated from NAA.
^ Northing and Easting coordinates from handheld GPS receiver; elevation from 1:50,000-scale topographic map. Otherwise, all measurements were made with a differentially corrected GPS receiver.
# Elevation of top of pit.

Table II. ^{14}C results from Cinca River terrace deposit.

		UA		CALIB 5.0[1]	
UA sample number	Project sample number	^{14}C yr BP	delta ^{13}C%	Intercepts	Preferred age (cal yr BP)[2]
AA53683	RCTA2-1-C2	15 177 ± 94	-5.52	18 109-18 386, 18 432-18 772	18 620
AA53684	RCTA2-1-C4	22 100 ± 160	-3.86		

[1]Calibrated using CALIB 5.0 as in Reimer et al., 2004.

Samples from soil pit RCTA2-1 at Ainsa (UTM N 4699550, UTM E 265500, elevation 529 m).

[2]Peak of intercept with higher relative area under probability distribution.

Table III: Summary of PDI values and B horizon development.

Soil Number	Location	Terrace[1]	PDI Value	B Horizon[2] Type	Carbonate Stage Morphology[3]
Cinca River					
RCT6-1	Belver	Qt5	59.9	Bk-Bkm	III$^+$
RCT6-2	Belver	Qt5	45.1	Bk-Bkm	IV$^+$
RCT6-3	Belver	Qt5	51.5	Bk-Bkm	IV$^+$
RCT5-1	Belver	Qt6	43.2	Btk	III$^+$
RCTM4-1	Monzón	Qt7	27.0	Btk	II
RCTM4-2	Monzón	Qt7	29.6	Btk	II
RCT4-1	Albalate	Qt7	31.5	Btk	II$^+$
RCT4-2	Albalate	Qt7	29.9	Btk-Bkm	III
RCTZ4-1	Almudafar	Qt7	33.3	Btk	II
RCT3-1	Albalate	Qt8	24.7	Btk-Bk	I$^+$
RCT3-2	Albalate	Qt8	23.2	Btk-Bk	I$^+$
RCTM2-1	Castejón	Qt9	14.7	Bwk-Bk	II$^+$
RCT2-1	Albalate	Qt9	18.1	Bwk	I$^-$
RCT1-1	Albalate	Qt10	5.6	Bw	0
Gállego River					
RGAT7-1	Sabiñánigo Alto	Qt5	58.2	Bt-Btk-Bk	I
RGAT7-2	Sabiñánigo Alto	Qt5	68.7	Btk-Bkm-Bk	III$^+$
RGIT7-1	Hostal de Ipiés	Qt7	28.1	Btk-Bk	II$^+$
RGAT9-1	Sabiñánigo	Qt7	33.1	Bt-Btk	II
RGLA9-1	Llano de Yeste	Qt7	30.9	Btk-Bk	II
RGM7-2	Murillo	Qt5	45.3	Btk-Bkm-Bk	III$^+$
RGAT2-1	Marracos	Qt8	22.3	Bwk-Bk	II
RGALA-11	La Peña	Qt9	13.0	Bk	I
SMOR-1	Senegüe		11.3	Bw	I
AMOR-1	Aurín		21.6	Btk-Bk	III

[1]Cinca River terrace number. For Gállego River, correlations with Cinca terraces are based on soil development.
[2]B horizons: w: color or structure B, k: accumulation of carbonates, t: accumulation of clay, m: cemented.
[3]Carbonate stage morphology from Gile et al. (1981), Birkeland (1999).

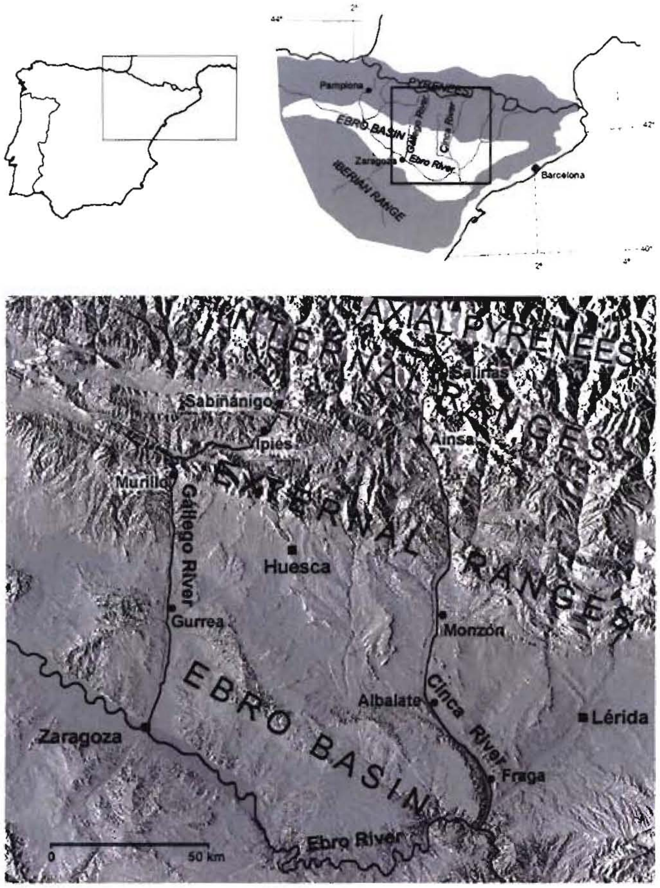
Pamplona
PYRENEES
EBRO BASIN
Gállego River
Cinca River
Zaragoza
Ebro River
IBERIAN RANGE
Barcelona
AXIAL PYRENEES
INTERNAL RANGES
Salinas
Sabiñánigo
Ipiés
Aínsa
Murillo
EXTERNAL RANGES
Gállego River
Huesca
Monzón
Gurrea
EBRO BASIN
Albalate
Cinca River
Lérida
Zaragoza
Fraga
Ebro River
0
50 km

Figure 1.

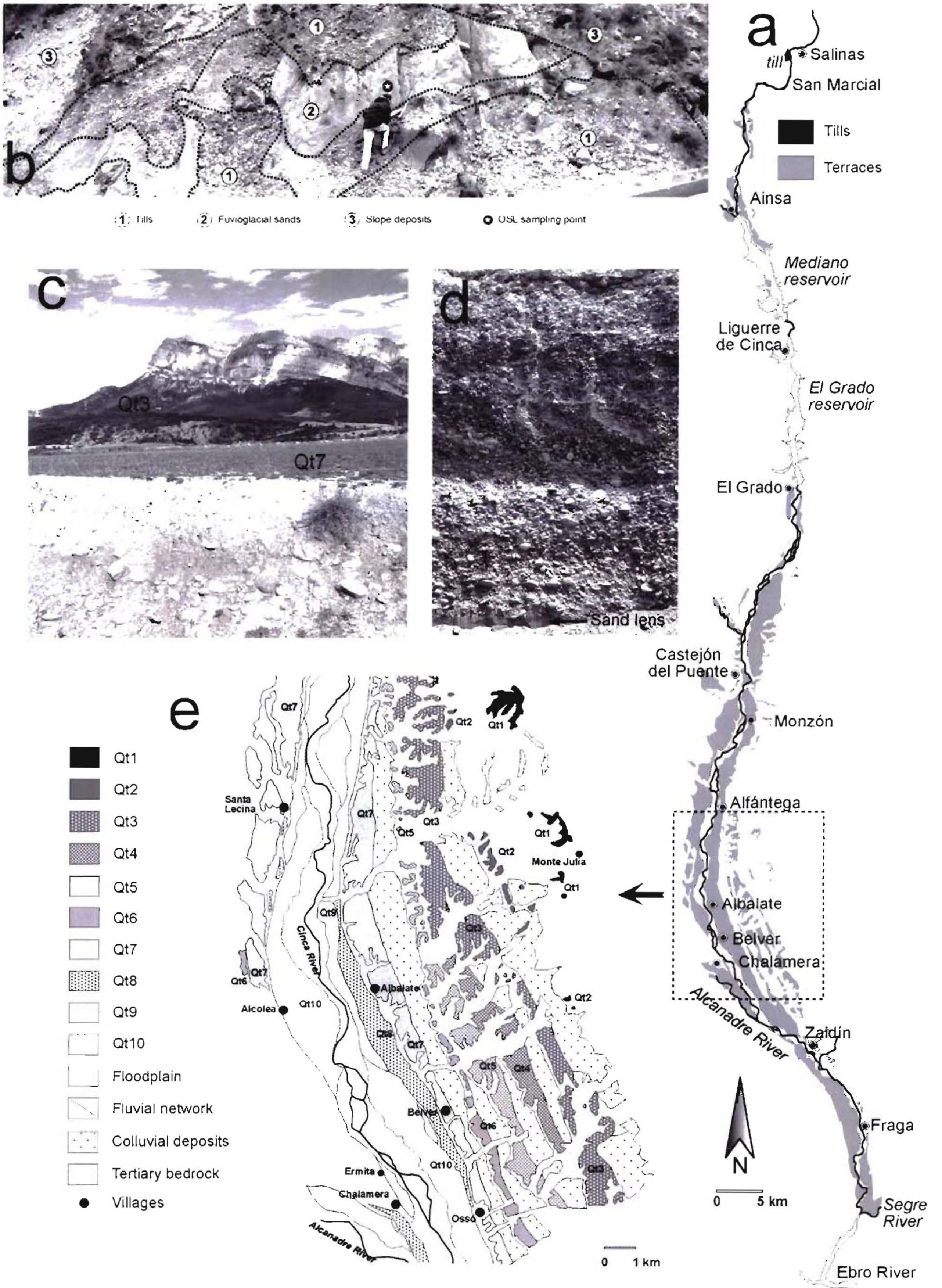
a
till
Salinas
San Marcial
Tills
Terraces
Ainsa
Mediano reservoir
Liguerre de Cinca
El Grado reservoir
El Grado
Castejón del Puente
Monzón
Alfántega
Albalate
Belver
Chalamera
Alcanadre River
Zaidín
Fraga
Segre River
Ebro River
N
0 5 km
b
1 Tills
2 Fluvioglacial sands
3 Slope deposits
OSL sampling point
c
Qt3
Qt7
d
Sand lens
e
Qt1
Qt2
Qt3
Qt4
Qt5
Qt6
Qt7
Qt8
Qt9
Qt10
Floodplain
Fluvial network
Colluvial deposits
Tertiary bedrock
Villages
Santa Lecina
Alcolea
Cinca River
Monte Julia
Albalate
Belver
Ermita
Chalamera
Ossó
Alcanadre River
0 1 km

Figure 2.

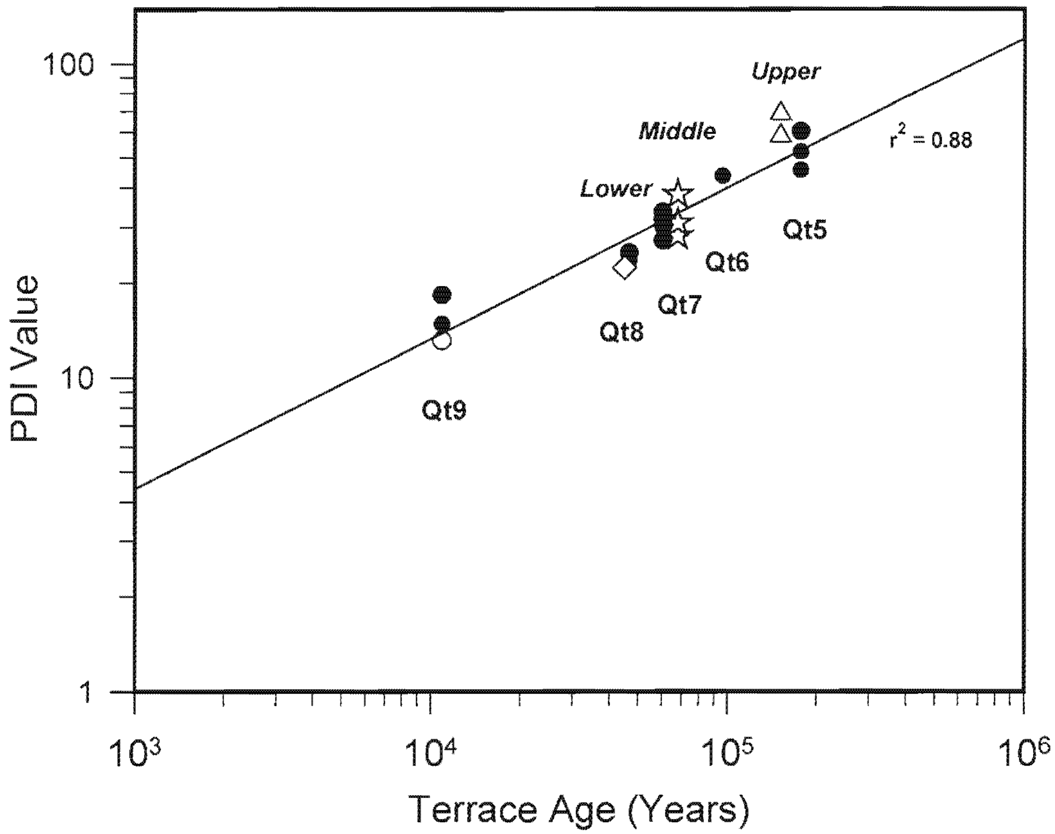

Upper
Middle
Lower
r^2 = 0.88
Qt5
Qt6
Qt7
Qt8
Qt9
PDI Value
Terrace Age (Years)
100
10
1
10^3
10^4
10^5
10^6

Figure 3.

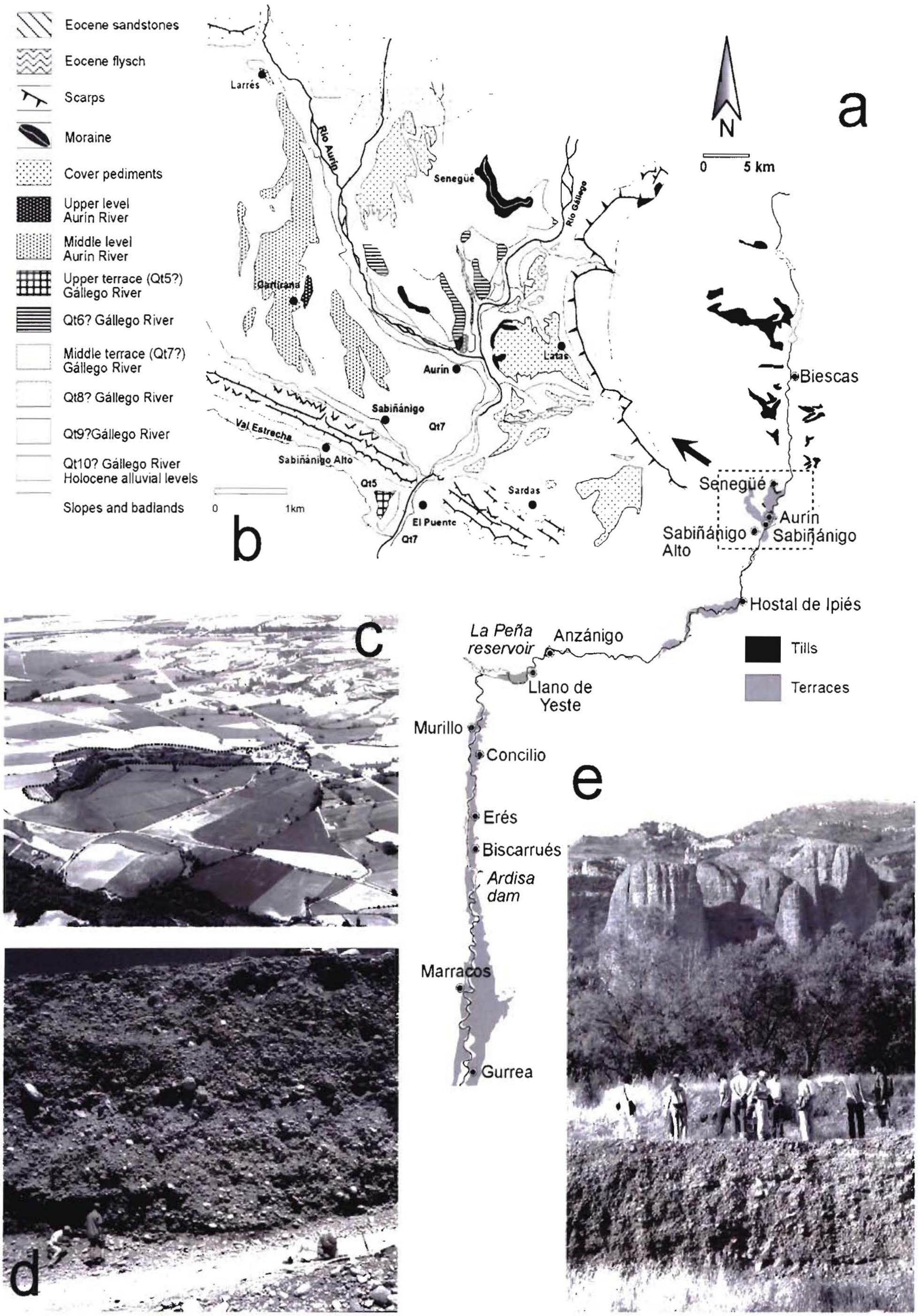

Eocene sandstones
Eocene flysch
Scarps
Moraine
Cover pediments
Upper level Aurín River
Middle level Aurín River
Upper terrace (Qt5?) Gállego River
Qt6? Gállego River
Middle terrace (Qt7?) Gállego River
Qt8? Gállego River
Qt9?Gállego River
Qt10? Gállego River Holocene alluvial levels
Slopes and badlands
0
1km
b
Larrés
Río Aurín
Senegüe
Río Gállego
Aurín
Latas
Sabiñánigo
Qt7
Val Estrecha
Sabiñánigo Alto
Qt5
Sardas
El Puente
Qt7
a
N
0
5 km
Biescas
Senegüé
Aurín
Sabiñánigo Alto
Sabiñánigo
Hostal de Ipiés
La Peña reservoir
Anzánigo
Llano de Yeste
Tills
Terraces
Murillo
Concilio
Erés
Biscarrués
Ardisa dam
Marracos
Gurrea
c
d
e

Figure 4.

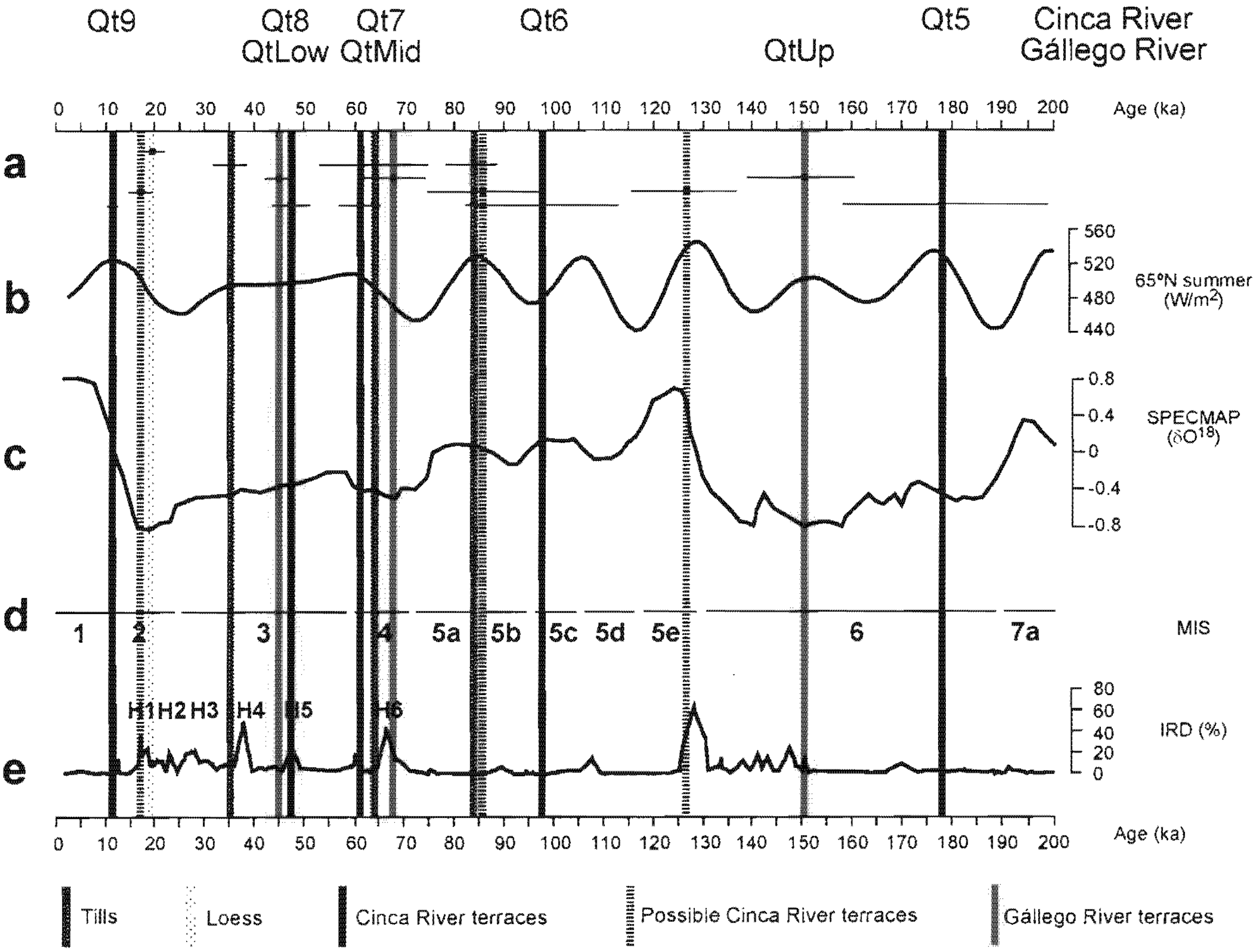
Qt9
Qt8
QtLow
Qt7
QtMid
Qt6
QtUp
Qt5
Cinca River
Gállego River
Age (ka)
a
b
c
d
e
65°N summer (W/m2)
SPECMAP (δO18)
MIS
IRD (%)
1
2
3
4
5a
5b
5c
5d
5e
6
7a
H1 H2 H3 H4 H5 H6
Tills
Loess
Cinca River terraces
Possible Cinca River terraces
Gállego River terraces

Figure 5.